Title
THE REACTIVE AND KINETIC PROPERTIES OF CARBON MONOXIDE AND CARBON DIOXIDE ON GRAPHITE SURFACE

Author
Marchon, B.

Publication Date
1987-10-01

LBL-24184
Preprint

Lawrence Berkeley Laboratory
UNIVERSITY OF CALIFORNIA

Materials & Chemical Sciences Division

Submitted to Journal of Physical Chemistry

The Reactive and Kinetic Properties of Carbon Monoxide and Carbon Dioxide on Graphite Surface

B. Marchon, W.T. Tysoe, J. Carrazza,
H. Heinemann, and G.A. Somorjai

October 1987

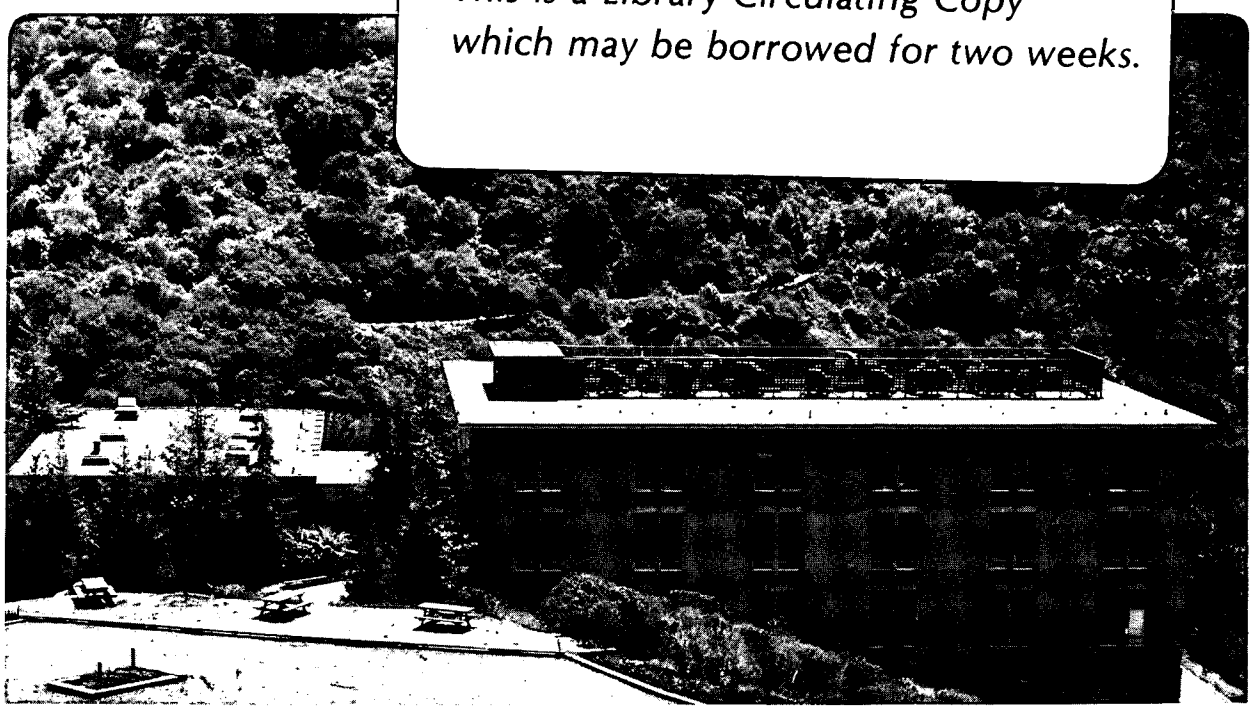

Prepared for the U.S. Department of Energy under Contract DE-AC03-76SF00098

DISCLAIMER

The Reactive and Kinetic Properties of Carbon Monoxide and Carbon Dioxide on Graphite Surface

B. Marchon[1,†], W. T. Tysoe[1,‡], J. Carrazza[1,2],
H. Heinemann[1,3] and G. A. Somorjai[1,2]

[1] *Materials and Chemical Sciences Division, Lawrence Berkeley Laboratory,* [2] *Department of Chemistry, and* [3] *Department of Chemical Engineering, University of California, Berkeley CA 94720, USA.*

Abstract

Temperature programmed desorption (TPD) results after chemisorption of carbon monoxide (CO) and carbon dioxide (CO_2) on polycrystalline graphite are presented. CO adsorbs onto graphite with a very low sticking coefficient ($< 10^{-12}$). After CO chemisorption, CO (mass 28 amu) desorbs in two temperature regions, between 400 and 700 K, and between 1000 and 1300 K, and CO_2 (mass 44 amu) desorbs below 950 K. The intensity of the CO_2 signal is less than one order of magnitude lower than the CO intensity. After CO_2 adsorption the major desorption product is CO at high temperatures (1000<T(K)<1300), whereas a small amount of CO_2 desorbs around 450 K. The adsorption of a $C^{16}O_2$ and $C^{18}O_2$ mixture leads to a nearly total oxygen scrambling of the CO_2 desorbed.

A mechanism for CO and CO_2 interconversion on the graphite surface is presented in term of surface oxide species, mainly lactones and semi-quinones, and their relative stability. Assignments of the TPD features is proposed accordingly.

Reaction studies on the CO_2 gasification of clean graphite and the CO disproportionation (Boudouard reaction) have been performed. A comparison between the activation energies obtained and the desorption energies calculated from the analysis of the TPD results indicate that both reactions are controlled by the desorption of the products.

†:Permanent address:Laboratoire de Spectrochimie Infrarouge et Raman, CNRS, 94320 Thiais, France.
‡:Permanent address:Department of Chemistry, University of Wisconsin, Milwaukee, WI 53211, USA.

1 Introduction

The surface oxides of a variety of carbon compounds such as carbon black, carbon fibers, coal and graphite have been extensively studied over the last two decades by an array of different methods. pH measurements [1], reactor studies [2], chemisorption kinetics [3,4], optical microscopy [5], thermal desorption under atmospheric pressure [6–13], and more recently new techniques like infrared absorption [14–15], nuclear magnetic resonance (NMR) [16] and surface science tools like X-ray photoelectron spectroscopy (XPS) [17–19], Auger electron spectroscopy (AES) [20–21] and temperature programmed desorption (TPD) [20–22] have brought some useful information an the nature of these surface species.

Most papers have dealt with the natural surface oxides or have studied oxidation of the clean surface (obtained after degassing at high temperatures) by O_2 or CO_2. All of them report a strongly bound surface complex that desorbs at temperatures higher than 1100 K as CO.

The nature of this oxide is not yet well understood although some evidence for a semi–quinone group has been observed [15,19]. Other groups such as carboxyls and lactones have also been proposed as possible candidates for graphite surface oxides [1,2,11,14].

To our knowledge, no work has been published on CO adsorption on graphite edge surfaces. The approach of this work has been to study the species produced

by the chemisorption of CO and CO_2 and their isotopic derivatives labelled with ^{13}C and ^{18}O onto a clean graphite sample under ultra high vacuum conditions. This permits the resulting surface species to be examined using a surface sensitive probe such as temperature programmed desorption (TPD). Experiments have been carried out on graphite samples from three different origins in order to check the reproducibility of the results. Also, kinetic measurements have been undertaken to study the interconversion of CO and CO_2 at the graphite surface (Boudouard equilibrium).

2 Experimental

In order to maximize the number of edge sites (which are the active chemisorption sites), three different kinds of finely dispersed polycrystalline graphite were used: two of them were commercial suspensions, one in isopropyl alcohol (Electrodag), and the other in water (Aquadag). The third sample was sintered machinable graphite which was finely ground and dispersed in hexane.

None of these samples is expected to be of maximum purity since they all contain a small amount of binder. In most cases, however, the binder is organic and very diluted. It is therefore likely to decompose at high temperatures.

The suspensions were deposited as thin films on a piece of tantalum foil. Tantalum was chosen for its high melting point (3269 K), low vapor pressure, good

mechanical properties and because it is coated with a very inert passivating oxide layer. The non-catalytic properties of tantalum toward graphite gasification were checked by running a reaction under flow reactor conditions with water vapor at 900 K. No carbonaceous compounds evolved. Blank TPD experiments were also carried out on the foil, without graphite, and no significant amount of CO or CO_2 adsorbed on the surface.

The sample was cleaned by annealing at ca. 1500 K for about 60 seconds. Neither XPS nor AES spectra showed an oxygen signal after the treatment. CO and CO_2 gases were of standard purity, and the ^{13}C and ^{18}O enriched compounds from Cambridge Isotope Laboratories were 98% pure.

The experiments were performed in a stainless steel diffusion pumped ultra high vacuum chamber. Additional titanium sublimation pumping allowed a base pressure of 5×10^{-10} Torr to be obtained after bakeout. Repeated adsorption-desorption cycles, however, led to working base pressures of 2×10^{-9} Torr.

The sample was mounted on a rotatable manipulator. It could be resistively heated and the temperature measured by means of a chromel-alumel thermocouple in intimate contact with the sample. A coaxial high pressure reactor was incorporated into the chamber so that the sample could be isolated from UHV and exposed to high pressure (up to 760 Torr) of CO or CO_2. The gases were circulated around an external loop in order to ensure that the reactants and products were well ho-

mogenized. It was found indispensible to bake out the loop for at least one hour before any gas introduction to avoid contamination by residual H_2O and O_2.

The rotatable manipulator allowed the sample to be turned toward a quadrupole mass spectrometer located 5 cm away from the sample for thermal desorption studies. TPD experiments were carried out using a heating rate of 50 K/sec.

In the kinetic studies, the reaction mixture was analyzed using a gas chromatograph equipped with a thermal conductivity detector sensitive to both CO and CO_2.

3 Results

The three different samples described above yielded similar results, although slight differences in TPD peak intensities were observed. Only results for the Aquadag samples will therefore be presented.

3.1 CO adsorption

The CO adsorption kinetics are presented in figure 1. The total CO desorption measured by integrating the mass 28 amu TPD peak is plotted versus exposure at various pressures.

The thermal desorption spectra taken after adsorption of 6×10^{-5} Torr of CO for 30 sec at different temperatures are plotted in figure 2. When adsorbed at 323 K, CO desorption occurs in two overlapping peaks at 393 and 503 K. Adsorption at higher

temperatures yields other TPD peaks at 673, 973 and 1093 K. Similar adsorption of ^{13}C showed no ^{12}CO evolved, i. e. no carbon exchange with the bulk occurs. Also, this allows us to rule out any O_2 or H_2O contaminations, which would lead to ^{12}CO desorption. Additional experiments performed with $C^{18}O$ confirmed this observation.

Some CO_2 (mass 44 amu) is produced after CO adsorption (figure 3). Room temperature adsorption leads to a single peak at 443 K, whereas higher adsorption temperatures lead to more stable species that desorb at 673 and 923 K. In our experimental conditions the amount of CO_2 desorbed after CO adsorption is always less than 10% of the total amount of CO chemisorbed.

3.2 CO_2 adsorption

The TPD spectra for mass 28 (^{12}CO), 29 (^{13}CO), 44 ($^{12}CO_2$) and 45 amu ($^{13}CO_2$) after adsorption of 8 Torr of $^{13}CO_2$ for 60 sec are reproduced in figure 4. Molecular $^{13}CO_2$ desorbs at 423 K. A large high temperature ^{12}CO TPD peak at 1093 K with two shoulders at 923 and 1253 K are observed. $C^{18}O_2$ adsorption resulted in identical desorption peaks at mass 30 amu ($C^{18}O$) indicating that there is no O_2 or H_2O contamination. Some ^{13}CO (mass 29 amu) is evolved at low temperature, and the weak mass 44 amu signal ($^{12}CO_2$) can be ascribed to isotopic impurities.

Adsorption of a 58–42% mixture of $C^{16}O_2$ and $C^{18}O_2$ leads to a nearly total scrambling on the surface as the CO_2 desorbed is 35% $C^{16}O_2$ (mass 44 amu), 41%

$C^{16}O^{18}O$ (mass 46 amu) and 24% $C^{18}O_2$ (mass 48 amu) (figure 5). Theoretical proportions for total scrambling are 34, 48 and 18% respectively.

3.3 Kinetic results

Reaction rates between CO and graphite and CO_2 and graphite were obtained using the high pressure reactor. Data for the C + $CO_2 \rightarrow$ 2 CO reaction as a function of temperature (plotted in Arrhenius form) is shown in figure 6. The slope of this line yields an activation energy of 67±3 kcal/mol. This value is in agreement although slightly higher, with that obtained in flow reactor experiments (59 kcal/mol) [23].

Figure 7 shows a similar plot for the reverse reaction: 2 CO $\rightarrow$ C + CO_2. In this case, rates were measured from the accumulation of CO_2, and the linear portion of the curve yields and activation energy for CO_2 formation of 24±2 kcal/mol.

4 Discussion

CO adsorbs onto graphite with a very low sticking coefficient. The mass 28 amu TPD peak obtained after adsorption of 100 Torr of CO for 30 sec is one order of magnitude smaller than the one obtained after O_2 adsorption [24]. Since it is well established that chemisorbed oxygen covers only a few percents of the total number of surface carbon atoms [3,6,22], it is clear that CO adsorption on graphite is a very low probability event, that is, highly activated. Its sticking probability is difficult to calculate, since the exact number of chemisorption sites in our polycrystalline

sample is unknown. The value can only be estimated to be of the order of 10^{-12} at room temperature, as 10^{10} Langmuir of exposure leads to a coverage of the order of a percent. Also, as observed in figure 1, it is highly pressure and coverage dependent.

Figure 2 shows that CO (mass 28 amu) desorbs in two temperature regions after CO adsorption. When CO is adsorbed at room temperature, desorption peaks at 393, 503 and 673 K are obtained, and when CO is adsorbed above 800 K, TPD peaks at 973 and 1093 K are observed. These results suggest that the two temperature regions are due to the desorption of two distinct surface species. The high temperature TPD feature is also observed after CO_2 adsorption (figure 6), and O_2 or H_2O oxidation [24] and it is therefore likely due to the same species. CO desorption peaks from carbon in the low temperature region have not been reported after adsorption of O_2, CO_2 or H_2O, but desorption of CO from metal surfaces usually occurs in this temperature region (400–700 K) [25].

Figure 4 shows that the major desorption product after CO_2 adsorption is CO at high temperatures. This figure also shows that the adsorption of $^{13}CO_2$ favors the desorption of ^{12}CO. This indicates the dissociation of CO_2, and the creation of a carbon-oxygen bond from the graphite lattice which would eventually desorb as ^{12}CO at high temperatures. This agrees with the mechanism proposed earlier by several authors [2,9,13]:

(1) $$^{13}CO_2 + {}^{12}C \longrightarrow {}^{12}C_S(O) + {}^{13}CO\uparrow$$

where the $^{12}C_s(O)$ is likely to be the same strongly bound species which is obtained after CO adsorption at high temperature (figure 2), owing to the similar desorption temperature. The above reaction implies the release of ^{13}CO, which can further adsorb on the surface. This is however a very low probability process, as discussed previously, and for this reason the area of the mass 29 amu peak in figure 6 is much lower than that of the mass 28 amu peak.

Assuming a frequency factor of 10^{13} sec^{-1}, Redhead's equation [26] can be used to obtain an estimate of the desorption energies from the peak temperatures in a TPD experiment. The values obtained for the CO and CO_2 species observed are summarized in Table I. A comparison between these values and the activation energy obtained in kinetic experiments for CO_2 gasification and the Boudouard reactions indicate that both reactions are controlled by the desorption of the products. The activation energy for CO_2 gasification, (67 kcal/mol) agrees well with the lowest desorption temperature for CO formation after CO_2 adsorption (around 64 kcal/mol), and the activation energy for the Boudouard reaction (24 kcal/mol) coincides with the lower limit in activation energy for desorption of CO_2 after CO adsorption (28 kcal/mol).

As mentioned in the introduction, there has been a great number of studies on the surface oxides adsorbed on various types of carbons. These studies, including spectroscopy, have proposed the existence of several types of surface groups. In

what follows, we will try to discuss in more details what chemical surface species are formed on the graphite surface after CO or CO_2 adsorption and that are responsible of the TPD peaks. As previously discussed, analysis of TPD data provides information about the desorption energy of the surface species involved, which is related to the strength of the bonds involved in the desorption process. By comparing these values with bond energies in similar organic compounds, we can make tentative assignments of the various desorption features to surface species.

It should be noticed, however, that it is difficult to get precise values of the bond energies on the graphite surface, from the desorption energies obtained from TPD. First, desorption energies are the sum of the activation energy for desorption and the surface bond energy. This activation energy is very low in the case of CO desorption on metal surfaces, for instance [25], but is known to be of the order of 10 kcal/mol [4] or greater [20] for O_2 on graphite. Also, Sanderson has pointed out [27] that the reorganizational energy of radicals after breaking the surface bond is an important contribution to the desorption energy, and in graphite this energy is expected to be considerable, because of the electron delocalization. Another complication to the determination of the bond strengths from TPD experiments is that the edges of the graphite particles contain various adsorption sites (zig-zag, arm-chair ...) that lead to species of different stability, whose desorption will multiply, or at least broaden the TPD features [28]. For example, theoretical calculations [29] have shown that

arm-chair sites are less reactive than zig-zag sites but are more stable.

Despite the complexity of the surface structure and the large number of variables involved in the desorption energy, we can reasonably assume that each surface species is likely to desorb in the same temperature range and that some qualitative trends can be established, which can help to the assignment of the TPD features to particular surface species. For example, it is easier to break external carbon-carbon bonds (~80 kcal/mol), than internal graphitic ones (~115 kcal/mol); and at temperatures below 1500 K, carbon-oxygen single bonds can be thermally dissociated (~85 kcal/mol), but double bonds cannot (~175 kcal/mol).

Taking into account all these considerations, the TPD features observed are assigned as follows. The low temperature CO desorption peaks at 393, 503 and 673 K, after exposure to CO at room temperature (figure 2) are likely due to weakly bound species such as carbonyl and/or cyclic ether groups.

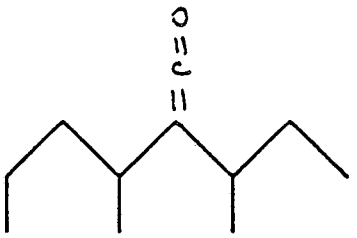

Carbonyl

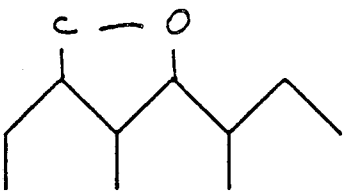

Ether

To our knowledge, carbonyl species adsorbed on carbon have never been cited in the literature before, but analogy with CO adsorption on single crystal metal surfaces [25] makes them favorable candidates. The transformation into ether groups

is only a ring closure and appears energetically favored. The lack of spectroscopic data, however, prevents any further answer. The mass 28 amu high temperature peaks between 923 and 1123 K, obtained after CO adsorption above 800 K, and CO_2 adsorption can be assigned to semi-quinone species adsorbed on various sites, like on a zig-zag edge as shown below:

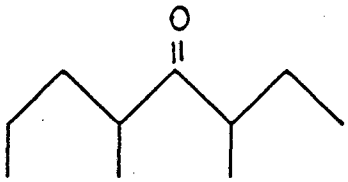

Semi-quinone

The high stability of quinone groups in polycyclic aromatic compounds [30] gives strong support to the existence of semi-quinones on the graphite surface. The desorption of this species involves the breaking of two graphitic carbon–carbon bonds from the lattice, and explains the high desorption temperature. In the case of ^{13}CO adsorption at high temperature, no ^{12}CO is evolved, indicating that CO does not dissociate on the surface, but it rather inserts onto the graphite lattice following the possible mechanism:

(2) 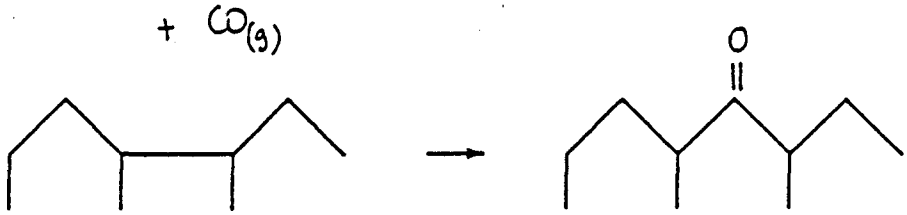

This insertion requires a graphitic carbon–carbon bond breaking, and it would explain why its formation is such a highly activated process.

At this point it is important to make a comment about the nomenclature used to identify these species. The name carbonyl has been employed to identify the low temperature CO species, rather than ketene, in agreement with IUPAC rules [31]. It must not be confused with the CO species desorbing above 1000 K after CO or CO_2 adsorption. Most authors refer to this highly stable species as carbonyl, but we prefer a more specific denomination, such as ketone or oxo [32], or better semi–quinone [33], to emphasize the strong conjugation with delocalized electrons as encountered in quinoid structures.

The formation of a semi-quinone group from CO_2 follows the previously described reaction (1), where the surface complex $C_S(O)$ is now better characterized:

(3) 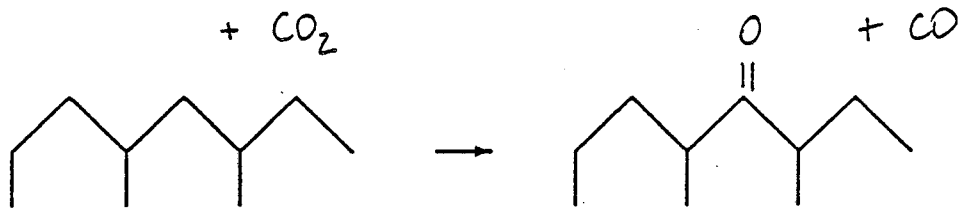

The desorption of CO_2 at 443, 673 and 923 K after CO adsorption is likely due to the thermal decarboxylation of a lactone group, which is a well known organic reaction taking place in the same temperature range [34]. The formation of these lactone functionalities from CO may imply semi-quinone groups as intermediates:

(4)

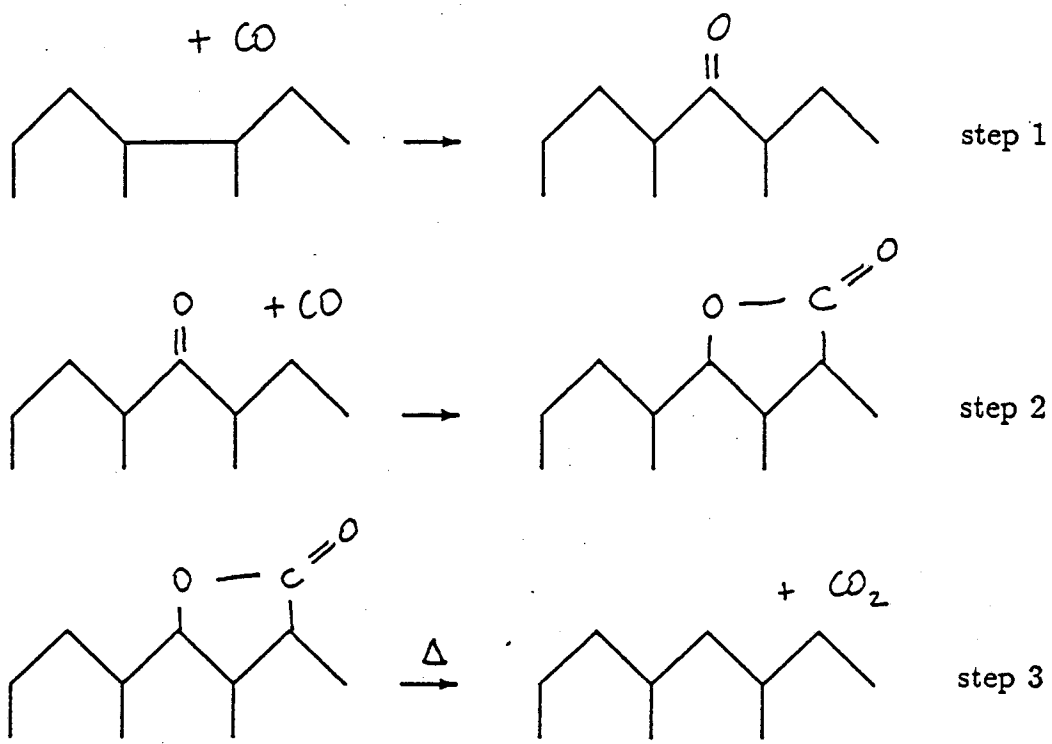

Again, a number of different sites are likely to give rise to such chemical species, and this explains the existence of several TPD 44 amu peaks in the low temperature region.

Equation (3) is simply the reverse reaction of equation (4) from step 3 to step 1, where step 2 has been omitted. The large number of semi-quinone groups formed after CO_2 adsorption as compared to lactones (figure 4) shows their greater stabilities as graphite surface species. The total oxygen scrambling that occurs when CO_2 is adsorbed (figure 5) may be explained by the kinetic equilibrium between the semi-quinone and the lactone groups of equation (4), and can be illustrated as follows:

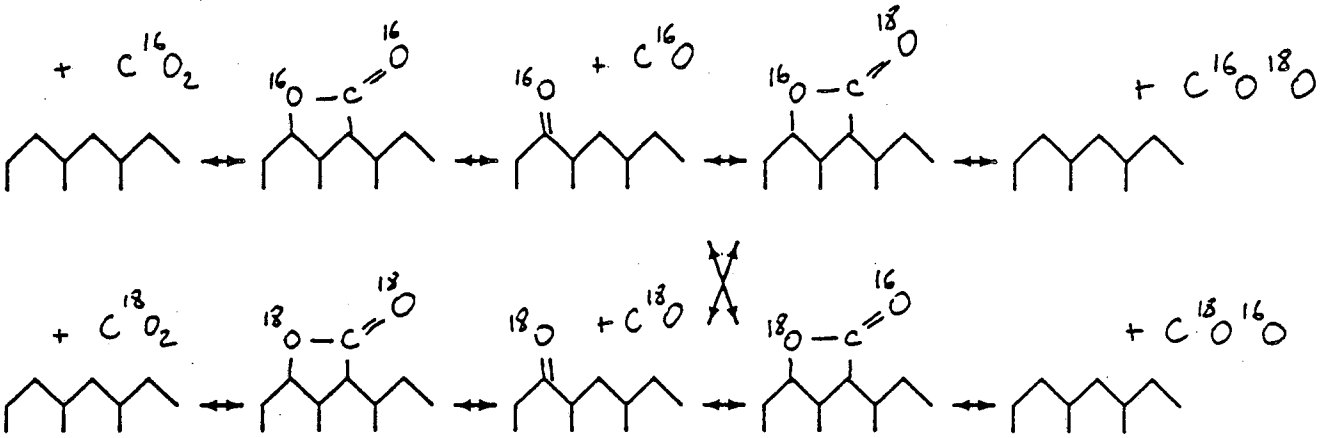

A summary of CO and CO_2 interconversion on the surface of graphite is shown in figure 8.

Other chemical groups like carbonates has been proposed as graphite surface oxides [14] and could account for the isotope scrambling as well. Such carbonates exist on a number of metal oxide surfaces [35] and are reasonable candidates for existing on the surface of graphite. At this point, we cannot rule out such species and more spectroscopic data should be gathered to clarify this. However, owing to the complexity of the system and the simplicity of our model which accounts for the experimental data, we will not discuss the existence of more elaborated structures.

5 Summary

The chemisorption and kinetic properties of CO and CO_2 adsorbed on graphite have been studied. Adsorption of CO is a highly activated process. It desorbs in two temperature regions, between 400 and 700 K, and between 1000 and 1200 K, suggesting the formation of two distinct groups of surface species, carbonyls and semi–quinones respectively. After adsorption of CO_2, CO is the main desorption product. Its desorption temperature is similar to that of the high temperature CO peak obtained after CO adsorption. This suggests that the same surface species, a semi-quinone, is formed in both cases. In the CO case this species is formed by incorporation of the CO in the graphite lattice, while in the CO_2 case it is formed by dissociation of CO_2 and transfer of one oxygen atom from the adsorbed gas onto the graphite lattice.

In both cases of CO and CO_2 adsorption at room temperature, CO_2 is desorbed between 423 and 443 K. In the CO case the amount of CO_2 desorbed is less than 10% of the amount of CO chemisorbed. In the CO_2 case the adsorption of a $C^{16}O_2$ and $C^{18}O_2$ mixture leads to a nearly total oxygen scrambling of the CO_2 desorbed. Surface lactone functionalities are proposed to account for this behavior.
We have evidence of various chemisorption sites (zig-zag, arm-chair ...) for a given surface species, according to several different TPD peak temperatures.

Reaction studies on the CO_2 gasification and CO disproportionation (Boudouard

reaction) have been performed. A comparison between the activation energies obtained and the desorption energies calculated from the analysis of the TPD results indicate that both reactions are controlled by the desorption of the products, i.e. the decomposition of the surface species.

Acknowledgements

This work was supported by the Assistant Secretary for Fossil Energy, Office of Management Planning and Technical Coordination, Technical Division of the U. S. Department of Energy under Contract Number DE-AC03-76SF00098, through the Morgantown Energy Technology Center, Morgantown W. VA. 26505

J. Carrazza acknowledges CEPET of Venezuela for a research fellowship.

References

1 - T.J. Fabish and D.E. Schleifer, Carbon, **22**, 19 (1984).

2 - P.D. Koenig, R.G. Squires, and N.M. Laurendeau, Carbon, **23**, 531 (1985).

3 - P.J. Hart, F.J. Vastola, and P.L. Walker, Carbon, **5**, 363 (1967).

4 - R.C. Bansal, F.J. Vastola, and P.L. Walker, J. Colloids and Inter. Sci., **32**, 187 (1969).

5 - H. Marsh and T.E. O'Hair, Carbon, **7**, 703 (1969).

6 - L. Bonnetain, J. Chim. Phys., **58**, 34 (1961).

7 - F.J. Vastola, P.J. Hart, and P.L. Walker, Carbon, **2**, 65 (1964).

8 - J. Dollimore, C.M. Freedman, B.H. Harrison, and D.F. Quinn, Carbon, **8**, 587 (1970).

9 - B.J. Tucker and M.F.R. Mulcahy, Trans. Farad. Soc., **65**, 274 (1969).

10 - F.S. Feates and C.W. Keep, Trans. Farad. Soc., **66**, 3156 (1970).

11 - S.S. Barton, G.L. Boulton, and B.H. Harrison, Carbon, **10**, 395 (1972).

12 - A. Sen and J.E. Bercaw, J. Phys. Chem., **84**, 465 (1980).

13 - J.A. Britten, J.L. Falconer, and L.F. Brown, Carbon, **23**, 627 (1987).

14 - C. Ishizaki and I. Marti, Carbon, **19**, 409 (1981).

15 - M.S. Akhter, J.R. Keifer, A.R. Chughtai, and D.M. Smith, Carbon, **23**, 589 (1985).

16 - C.A. Mims, K.D. Rose, M.T. Melchior, and J.K. Pabst, J. Am. Chem. Soc, **104**, 6886 (1982).

17 - D.L. Perry and A. Grint, Fuel, **62**, 1024 (1983).

18 - D.T. Clark and R. Wilson, Fuel, **62**, 1034 (1983).

19 - T. Tagahagi and I. Ishitani, Carbon, **22**, 43 (1984).

20 - S.R. Kelemen and H. Freund, Carbon, **23**, 619 (1985).

21 - S.R. Kelemen and H. Freund, Carbon, **23**, 723 (1985).

22 - S.S. Barton, B.H. Harrison, and J. Dollimore, J. Phys. Chem., **82**, 290 (1978).

23 - S. Ergun, J. Phys., Chem., **60**, 480 (1956).

24 - B. Marchon, J. Carrazza, H. Heinemann, and G.A. Somorjai, to be published.

25 - G.A. Somorjai, Chemistry in two dimensions: Surfaces, Cornell University Press, Ithaca, London (1981).

26 - P.A. Redhead, Vacuum, **12**, 203, (1962).

27 - R.T. Sanderson, Chemical bond in organic compounds, Sun and Sand Publishers, Scottsdale, Arizona (1976).

28 - R.N. Smith, D.A. Young, and R.A. Smith, Trans. Farad. Soc., **62**, 2280 (1966).

29 - S.E. Stein and R.L. Brown, Carbon, 23, 105 (1985).

30 - E. Clar, Polycyclic aromatic hydrocarbons, Academic Press (1964).

31 - IUPAC, Nomenclature of organic chemistry, Pergamon Press (1979), Rule C321.2.

32 - Idem, Rule C.3.1.

33 - V.A. Garten, D.E. Weiss, and J.B. Willis, Aust. J. Chem., 10, 295 (157).

34 - W. Adam, J. Baeza, and J.C. Liu, J. Am. Chem. Soc., 94, 2000 (1972).

35 - M.L. Hair, Infrared spectroscopy in surface chemistry, E. Arnold Publisher (1967) p.204 .

Figure captions

Figure 1 : CO adsorption kinetics on polycrystalline graphite at room temperature. The CO coverage is estimated from the integrated intensity of the 28 amu low temperature TPD peak.

Figure 2 : TPD spectra, mass 28 amu, after CO adsorption ($6x10^{-5}$ Torr for 30 sec.) on polycrystalline graphite at various temperatures.

Figure 3 : TPD spectra, mass 44 amu, after CO adsorption ($6x10^{-5}$ Torr for 30 sec.) on polycrystalline graphite at various temperatures.

Figure 4 : TPD spectra after $^{13}CO_2$ adsorption (8 Torr for 60 sec.) on polycrystalline graphite at room temperature.

Figure 5 : TPD spectra after adsorption ($2x10^{-4}$ Torr for 30 sec.) of a 58% $C^{16}O_2$ - 42% $C^{16}O_2$ mixture on polycrystalline graphite at room temperature. In insert is the mass spectrum of the mixture; mass 46 amu peak is ascribed to isotopic impurity.

Figure 6 : Arrhenius plot for the reaction $C + CO_2 \rightarrow 2\ CO$ performed in the high pressure cell.

Figure 7 : Arrhenius plot for the reaction $2\ CO \rightarrow C + CO_2$ performed in the high pressure cell.

Figure 8: Simplified model for CO and CO_2 interconversion on a graphite surface.

Some energy ranges deduced from our experiments are indicated. The ordinate units are arbitrary and the relative energy level of the surface compounds are not respected.

Table I: Desorption products and energies of desorption of CO and CO_2 adsorbed on graphite .

Adsorption gas	Adsorption temp (K)	Desorption product	Desorption temp (K)	E_{des} kcal/mol	Assignment
CO CO_2	> 800 room temp	CO	973–1253	64–83	semi-quinones
CO	325–600	CO	400–700	25–44	carbonyls
CO CO_2 CO	room temp room temp 400–750	CO_2	443 423 443–923	28 27 28–60	lactones

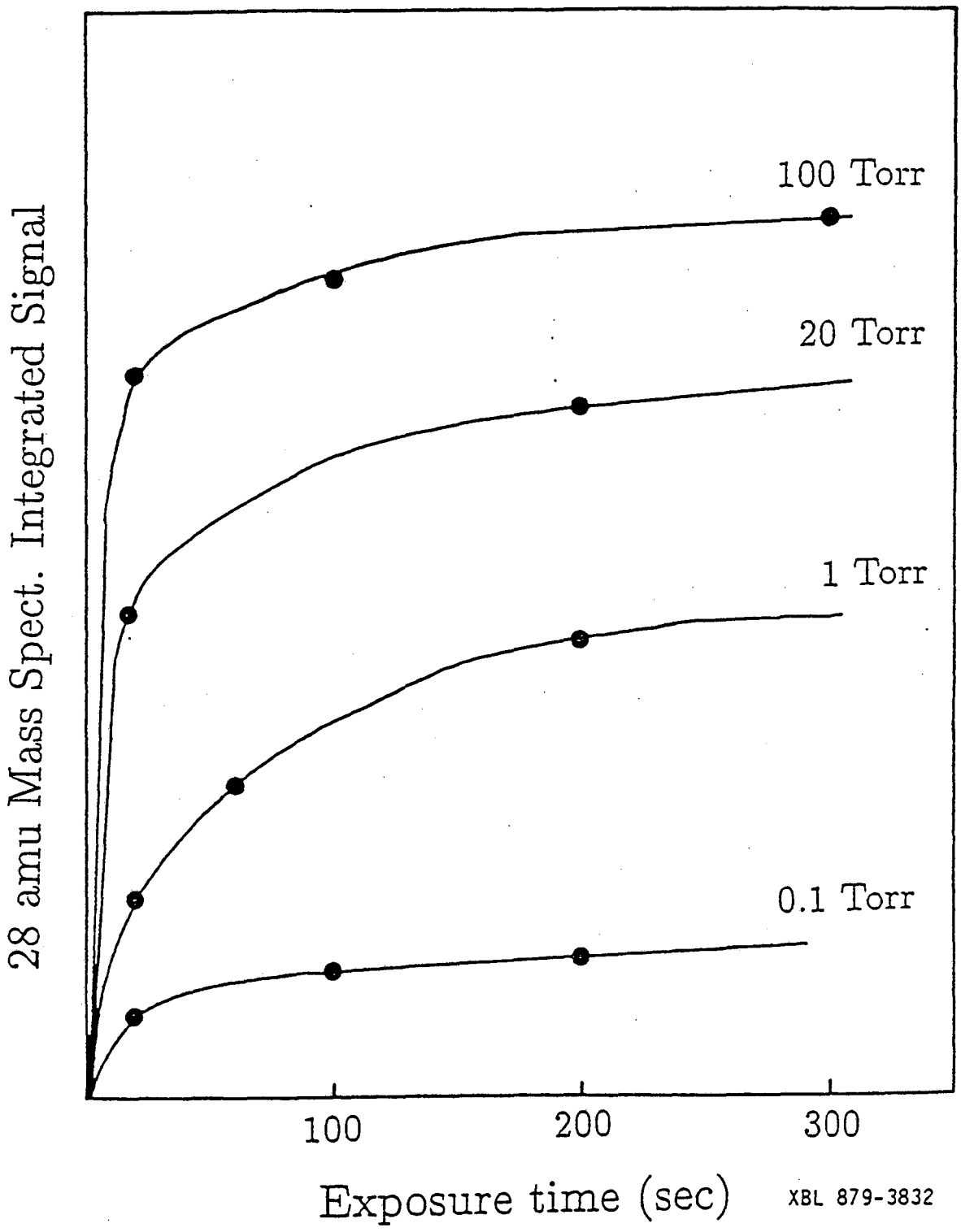
100 Torr
20 Torr
1 Torr
0.1 Torr
28 amu Mass Spect. Integrated Signal
100
200
300
Exposure time (sec)
XBL 879-3832

Figure 1

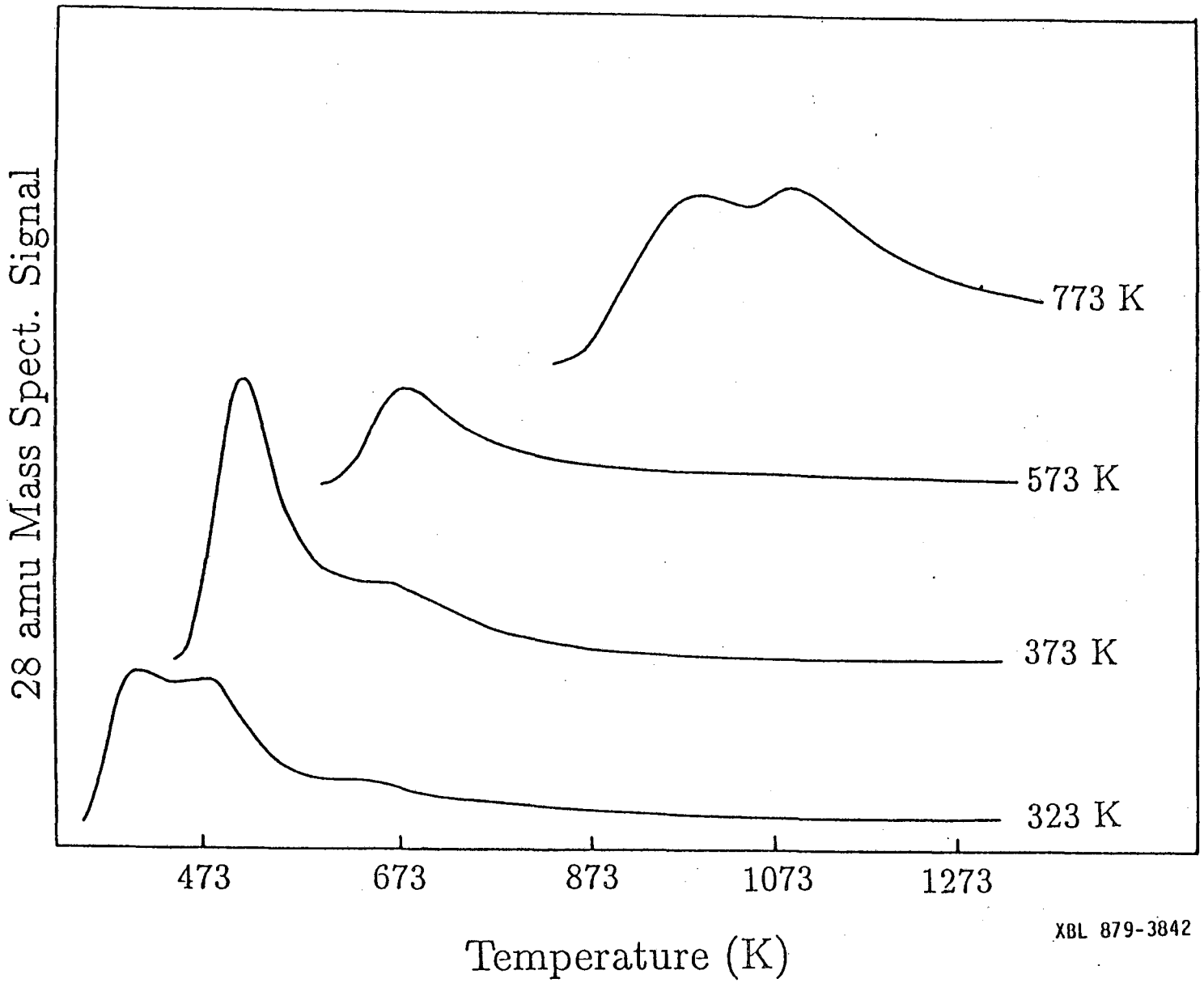
28 amu Mass Spect. Signal
773 K
573 K
373 K
323 K
473
673
873
1073
1273
Temperature (K)
XBL 879-3842

Figure 2

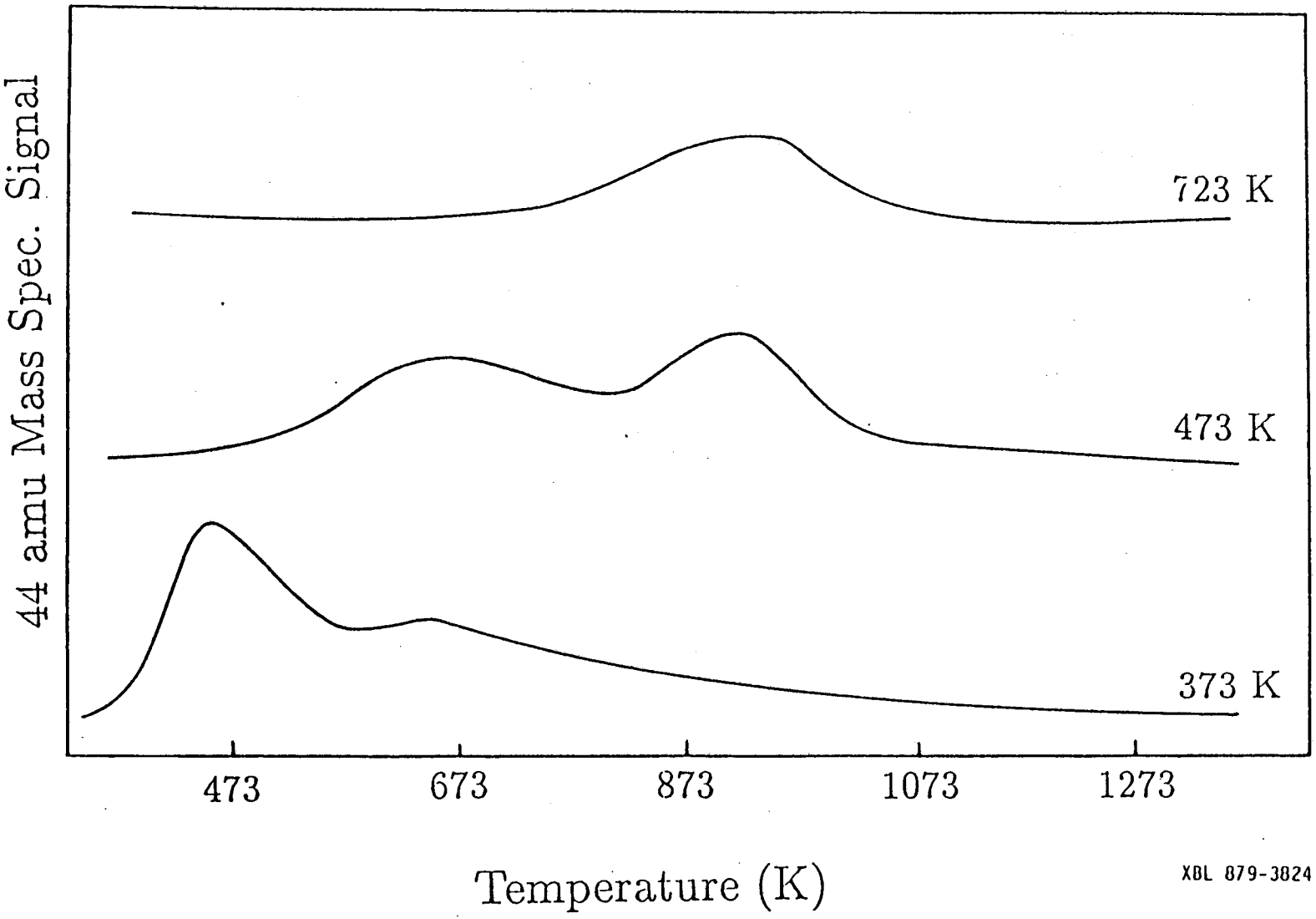
44 amu Mass Spec. Signal
723 K
473 K
373 K
473
673
873
1073
1273
Temperature (K)
XBL 879-3824

Figure 3

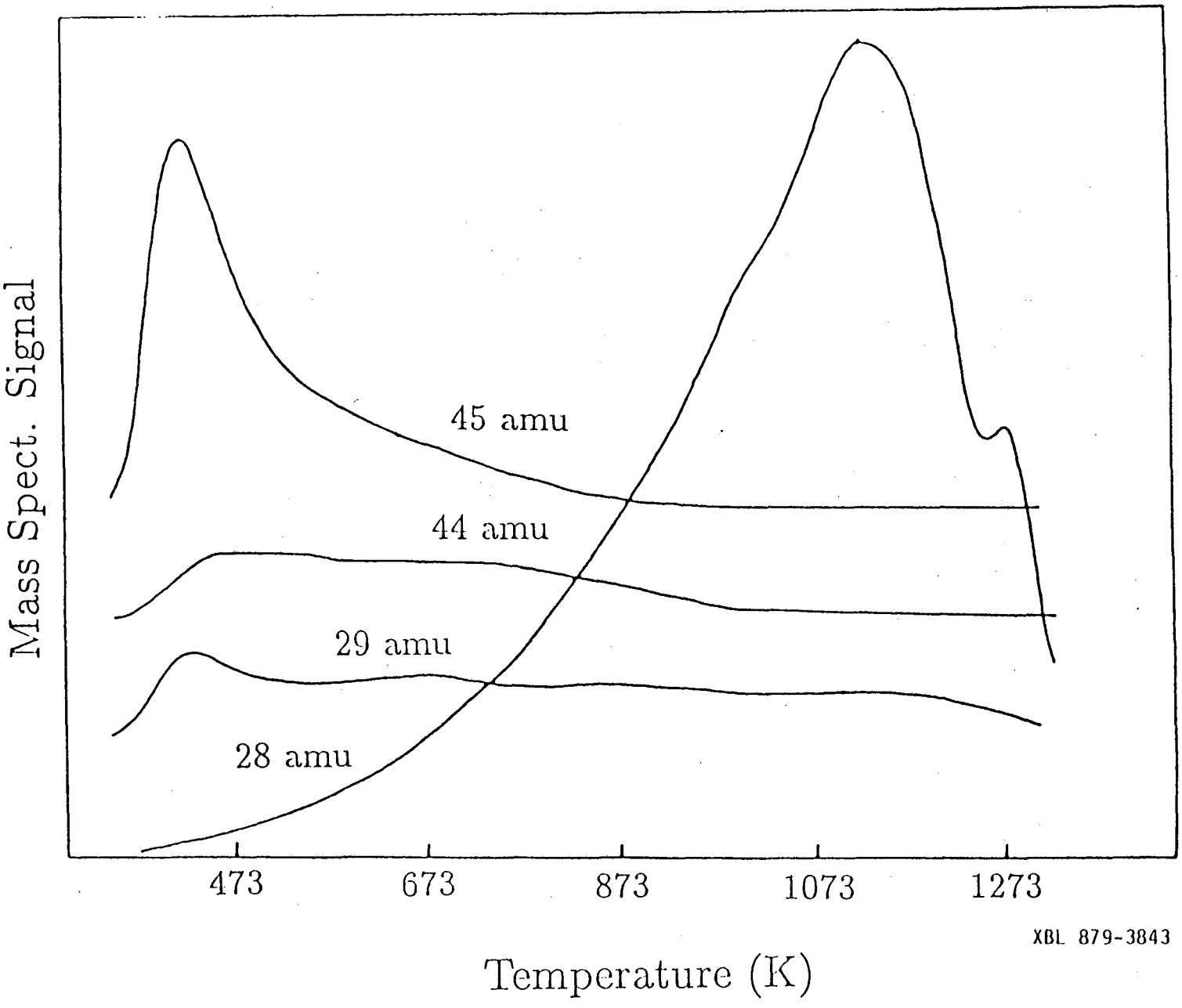
Mass Spect. Signal
45 amu
44 amu
29 amu
28 amu
473
673
873
1073
1273
XBL 879-3843
Temperature (K)

Figure 4

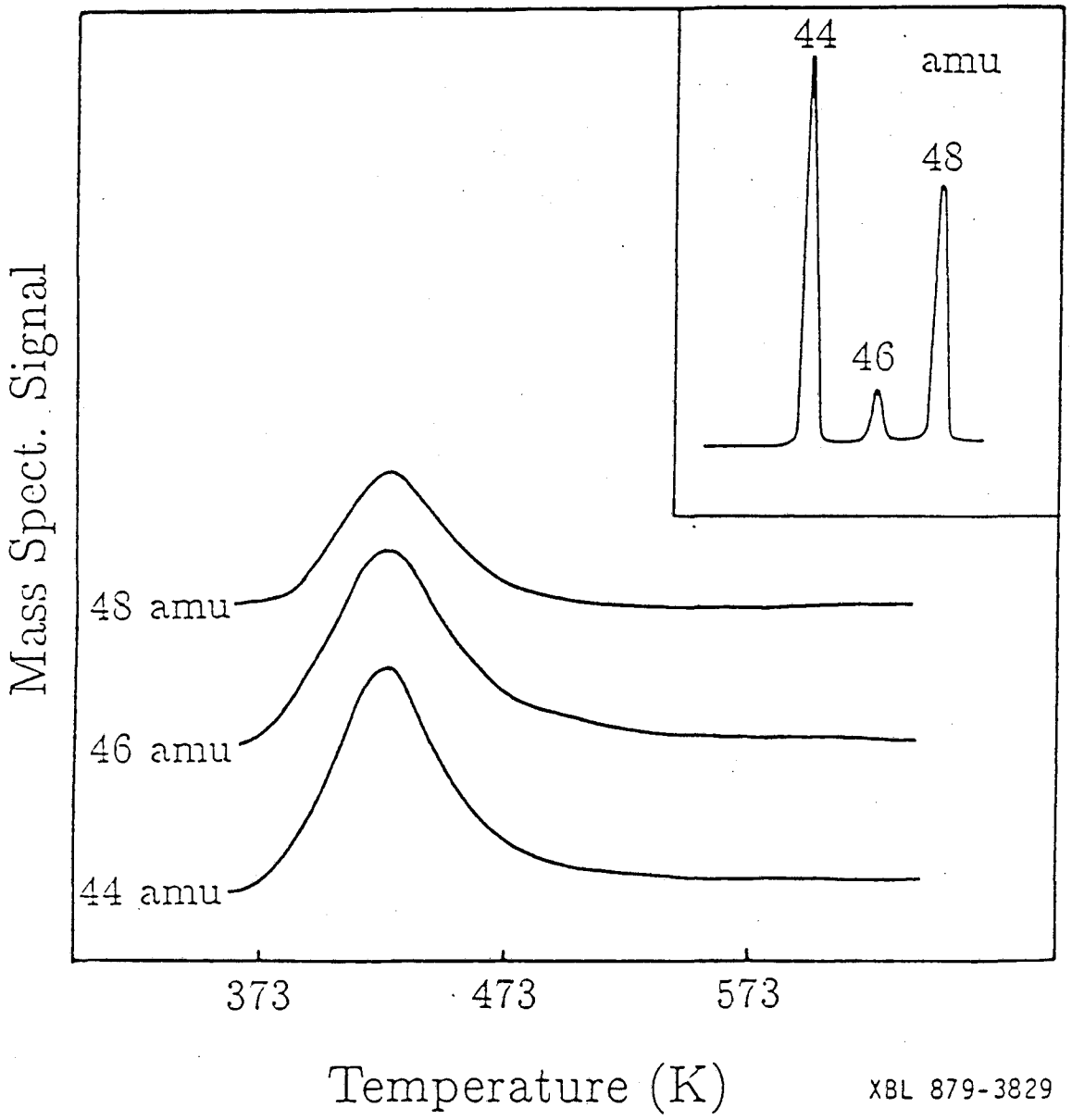
44
amu
48
46
Mass Spect. Signal
48 amu
46 amu
44 amu
373
473
573
Temperature (K)
XBL 879-3829

Figure 5

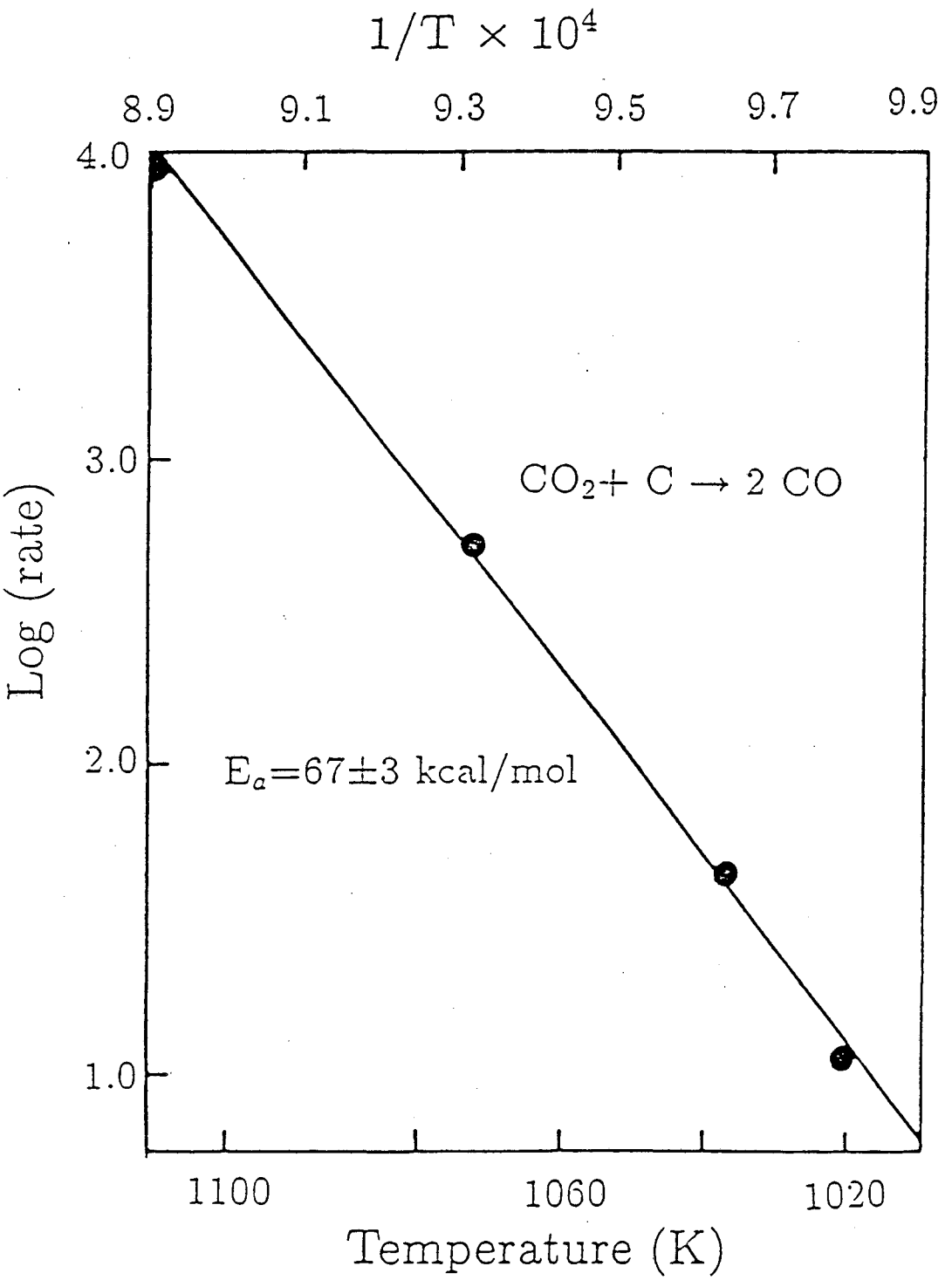

XBL 879-3827

Figure 6

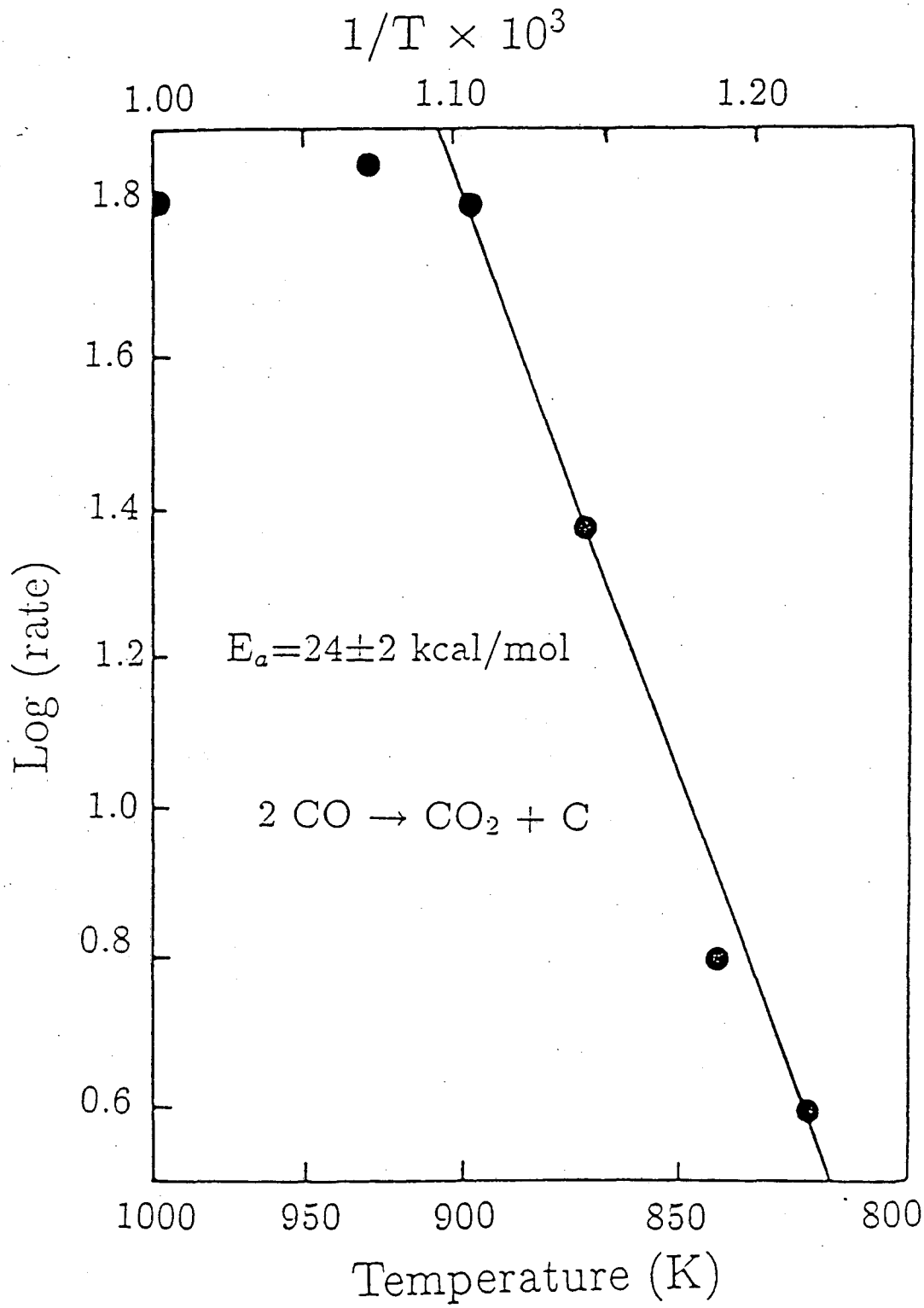

XBL 879-3826

Figure 7

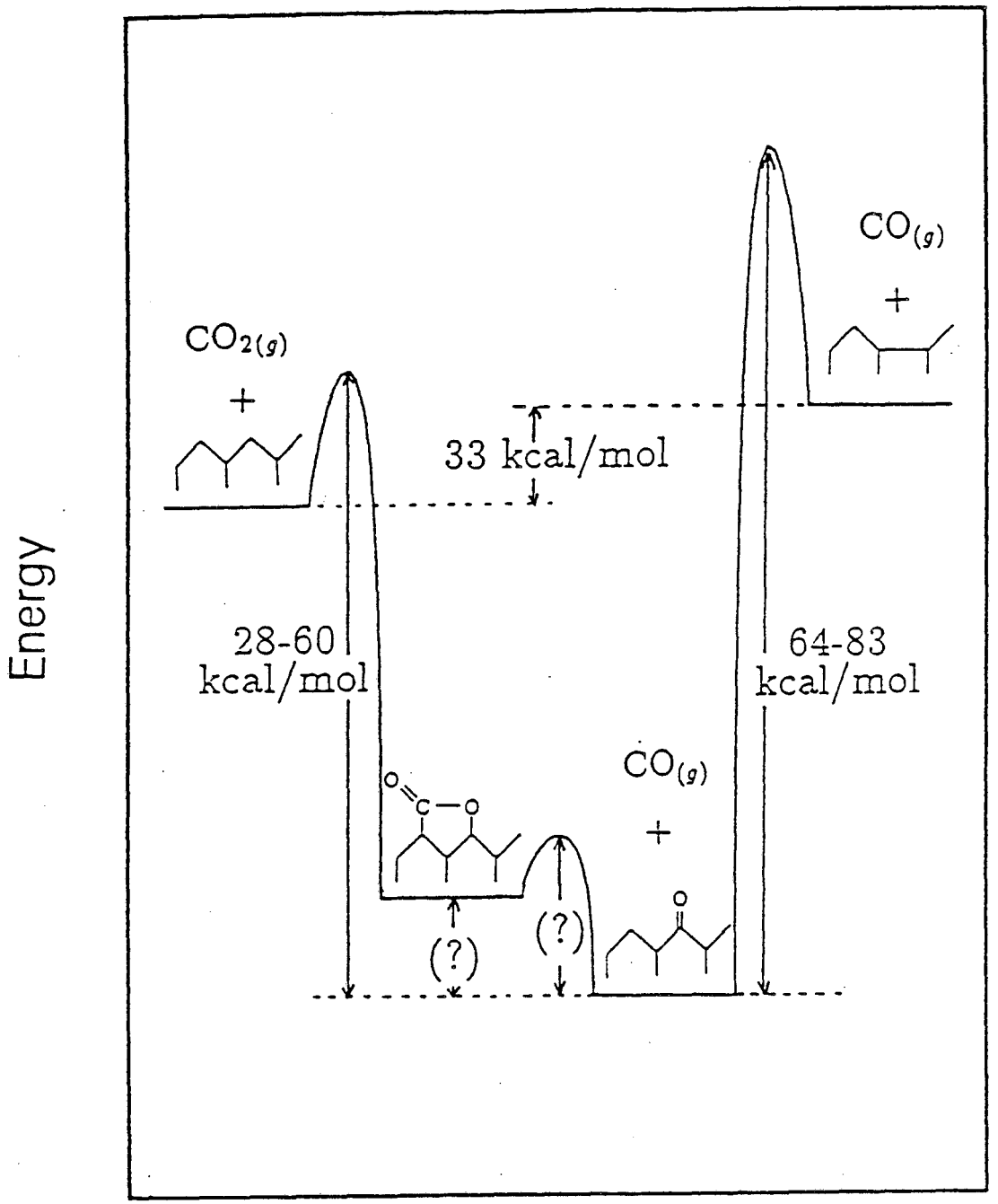

XBL 879-3894

Figure 8

LAWRENCE BERKELEY LABORATORY
TECHNICAL INFORMATION DEPARTMENT
UNIVERSITY OF CALIFORNIA
BERKELEY, CALIFORNIA 94720